Numerical Modeling of Space Plasma Flows

ASTRONUM-2009

Chamonix-Mont-Blanc, France

June 29 – July 3, 2009

Prgholqj#kholrvskhulf#skhqrphqd#zlwk#wkh#
pxowl0vfdoh#ioxlg0nlqhwlf#vlpxodwlrq#vxlwh

N. V. Pogorelov
Department of Physics and Center for Space Physics and Aeronomic Research,
University of Alabama in Huntsville, U.S.A.

Acknowledgments to S.N. Borovikov, J. Heerikhuisen, I.A. Kryukov, and G.P. Zank

Talk overview

1. **SW – LISM interaction: colliding streams of partially ionized plasma.**
2. **MS-FLUKSS structure**
3. **Comparison of MHD-kinetic and multi-fluid simulations.**
4. **Modeling vs. Voyager observations.**
5. **The importance of time dependent b.c. in the solar wind.**
6. **Conclusions.**

Properties of the solar wind and the local interstellar medium

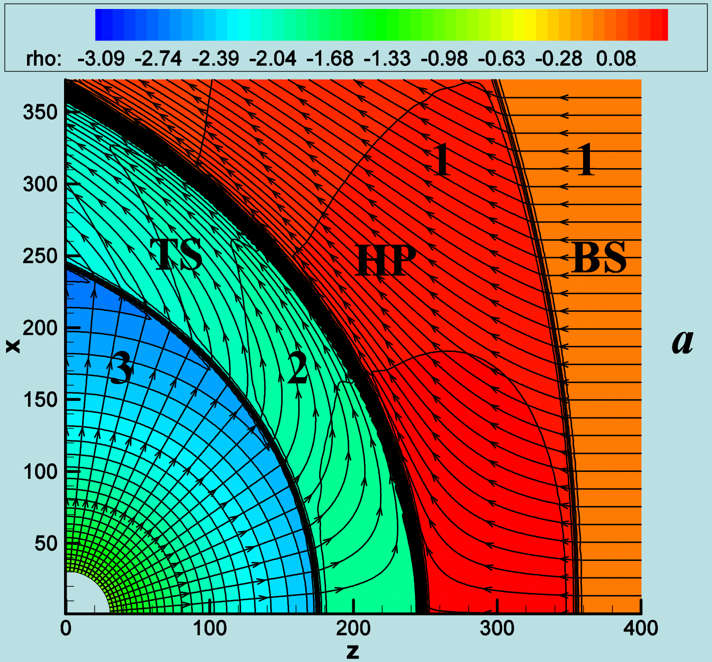

Solar wind:

V_p = 450 km/s, n_p = 7.4 cm^{-3}, and T_p = 51100 K.

LISM:

V_∞ = 26.4 km/s, n_∞=0.05 – 0.07 cm^{-3},
T_∞ = 6500 K, $n_{H\infty}$ = 0.15 – 0.18 cm^{-3}.

Neutral particles play a major role in the SW-LISM interaction (Wallis 1971, 1975; Baranov & Malama 1993; Zank et al., 1996; Fahr et al. 2000; Florinski et al. 2003; Izmodenov et al., 2005; Heerikhuisen et al., 2006, 2007, 2008, Pogorelov et al. 2006, 2007, 2008, 2009).

We model the transport on neutral particles kinetically. The distribution of ions is assumed to be Lorentzian with κ = 1.63, rather than being Maxwellian.

The system of MHD equations in the symmetrizable Godunov's form with the charge-exchange/collisional terms

$$\frac{\partial}{\partial t}\begin{bmatrix}\rho\\ \rho\mathbf{v}\\ e\\ \mathbf{B}\end{bmatrix} + \nabla\cdot\begin{bmatrix}\rho\mathbf{v}\\ \rho\mathbf{v}\mathbf{v}+p_0\hat{\mathbf{I}}-\dfrac{\mathbf{B}\mathbf{B}}{4\pi}\\ (e+p_0)\,\mathbf{v}-\dfrac{\mathbf{B}(\mathbf{v}\cdot\mathbf{B})}{4\pi}\\ \mathbf{v}\mathbf{B}-\mathbf{B}\mathbf{v}\end{bmatrix}$$

$$= -\begin{bmatrix}0\\ \dfrac{\mathbf{B}}{4\pi}\\ \dfrac{\mathbf{v}\cdot\mathbf{B}}{4\pi}\\ \mathbf{v}\end{bmatrix}\times\nabla\cdot\mathbf{B}+\begin{bmatrix}0\\ \mathbf{H}^{\mathrm{m}}_{\mathrm{p-H}}\\ H^{\mathrm{e}}_{\mathrm{p-H}}\\ 0\end{bmatrix}.$$

Collisional terms are derived from the kinetic transport equations for the protons and neutral species, and we use either pitch-angle averaged or differential cross-sections for corresponding processes. For example, using stochastic Monte Carlo simulations (Baranov & Malama 1993; Izmodenov et al. 2005; Heerikhuisen et al. 2006, 2007).

In a multi-fluid model, collisional terms in the Boltzmann equations are first integrated in the velocity spaces of plasma and neutral particles in the assumption of the Maxwellian (or other) distribution function for all populations. Then the zeroth, first, and second moments of the source terms are taken, giving us the source terms in the mass, momentum , and energy equations of the ideal MHD or Euler system. The number of the Euler systems to be solved is equal to the number *M* of neutral fluids involved in the model times the number *N* of populations for each of the fluids.

P V0IOXNVV=#P xowl0Vfdoh#Ioxlg0Nlqhwlf#Vlpxodwlrq#Vxlwh
+vxssruwhg#e|#QDVD#dqg#QVI,

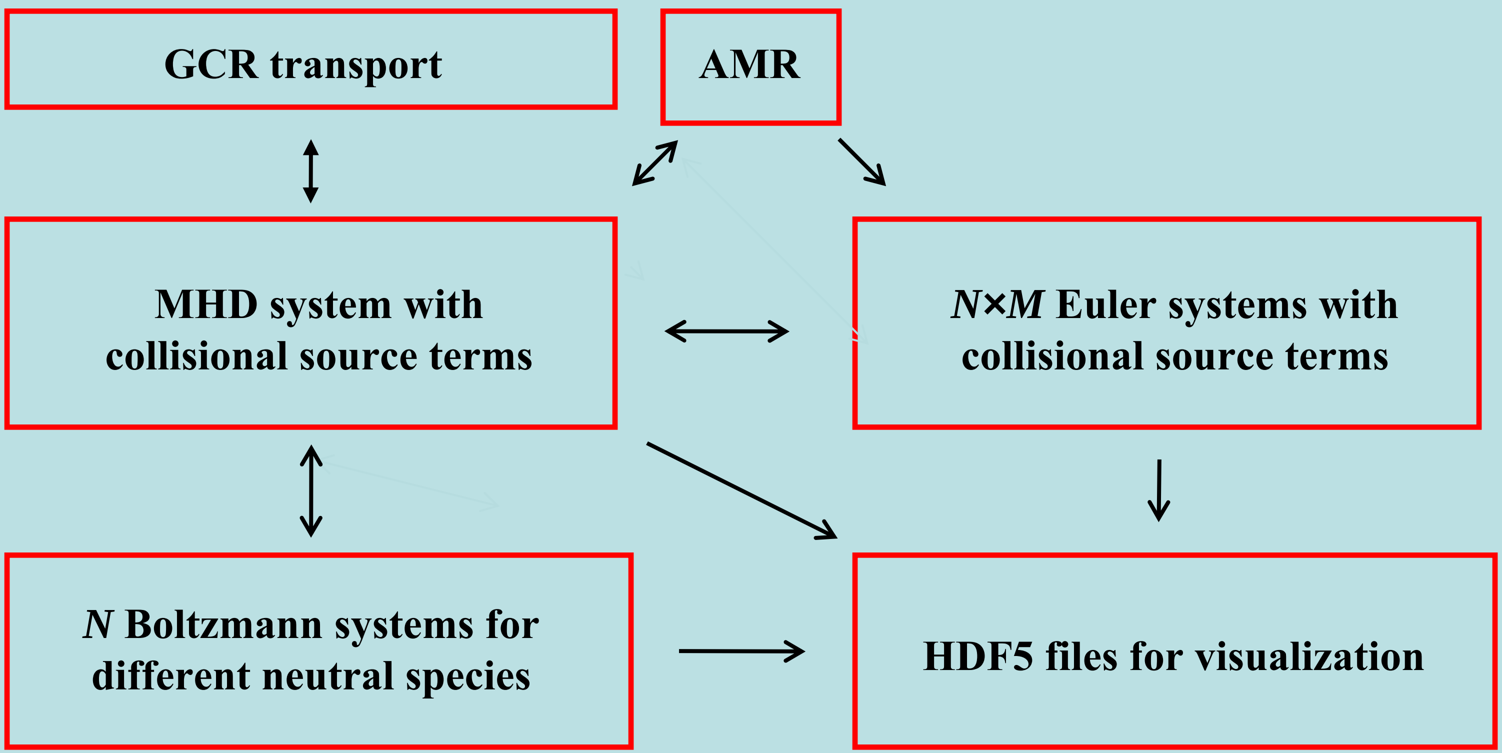

The reason of using DSMC: the mean free-path of neutral H with respect to charge exchange with ions is comparable with characteristic sizes of the regions where collisions take place.

The approach is perfect, but time consuming for unsteady flows. If you need to perform DSMC at small time steps, the number of particles to be involved should be increased to accumulate a satisfactory statistics. An example: unstable HP.
An alternative to the DSMC approach is a 5-fluid approach.

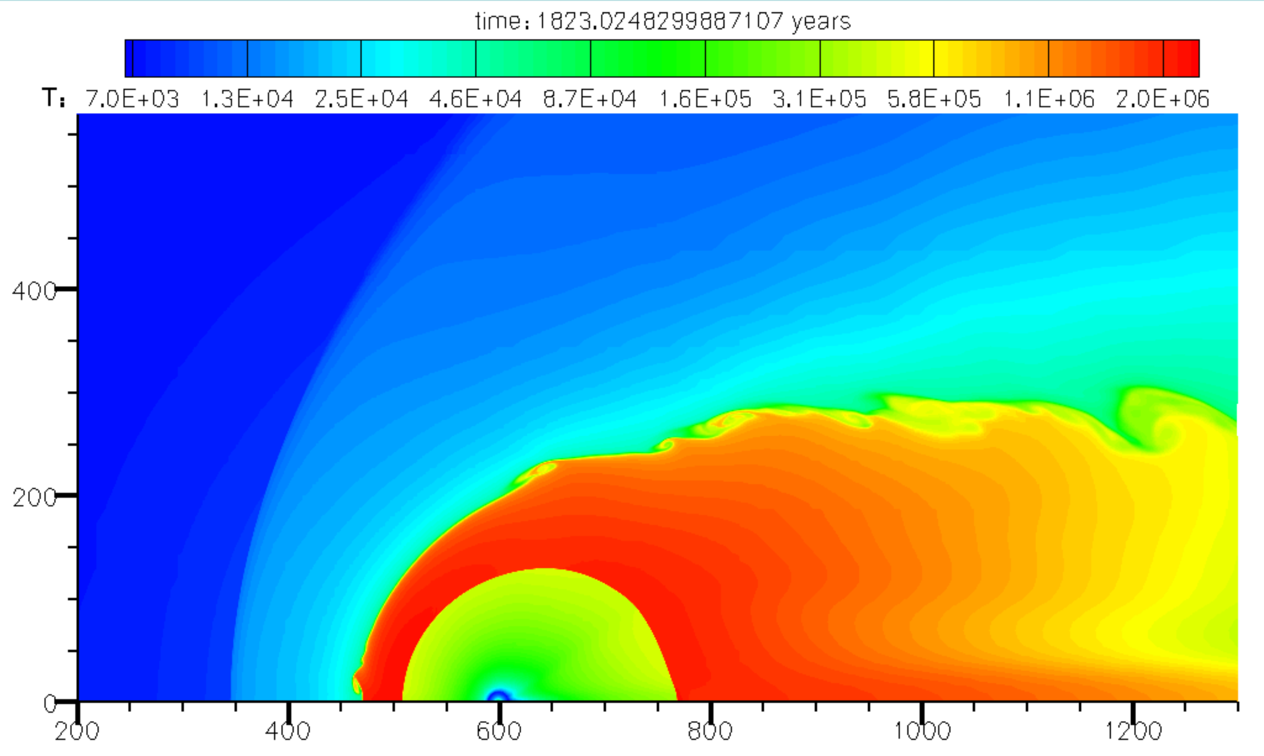

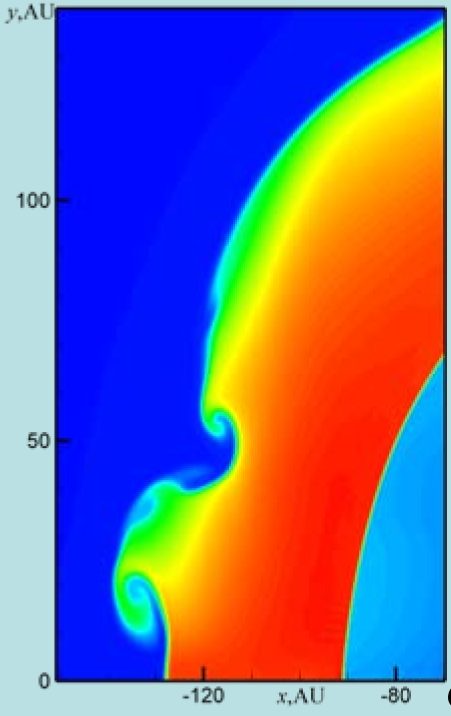

Methods implemented

The Euler equations:

1. Roe's finite-volume method of the 2nd order of accuracy in space and time (using either the Runge – Kutta or MUSCL-Hancock schemes).
2. Subsonic outflow boundary conditions based on the Osher – Matsuda – Pogorelov & Semenov approach, which allows us to substantially decrease the size of the computational region.
3. Charge-exchange source terms are treated explicitly for every fluid.
4. Nonlinear reconstruction of the characteristic variables.
5. AMR grid is provided from the analysis of the plasma flow and/or geometrical considerations.
6. Implemented for orthogonal, curvilinear, AMR grids.

MHD equations:

1. TVD Courant – Isaacson – Rees, Roe's, and Lax – Friedrichs methods are implemented with the 2nd order of accuracy both in space and time.
2. Divergence cleaning is ensured by the Powell's, CT techniques (Balsara; Gardiner & Stone), projection method based on the Poisson solver provided by the latest release of Chombo).
3. Subfast exit boundary conditions allow us to reduce the size of the computational region.
4. The Riemann problem is solved either with an 8-wave (Brio & Wu, 1988) or 7-wave (Pogorelov & Semenov, 1995) solvers.
5. The source terms are treated explicitly, being provided by either the multi-fluid or kinetic component of the package. The ionized component is either Maxwellian or Lorenzian.
6. AMR, parallelization, and processor load balancing is provided by Chombo.
7. We developed modules allowing us to use orthogonal, curvilinear grids.

Data handling and visualization:

1. Storing data in Hierarchical Data Format (HDF5) allows us restarting the code on any computer platform with any number of processors. HDF5 also provides tools for managing, manipulating, viewing, and analyzing data.
2. Tecplot can be efficiently used only for 2D images. We mostly use VisIt to visualize the results of our large-scale simulation. VisIt allows us to perform remote, parallel analysis of data files as large as 400 Gb.

The Orszag – Tang problem

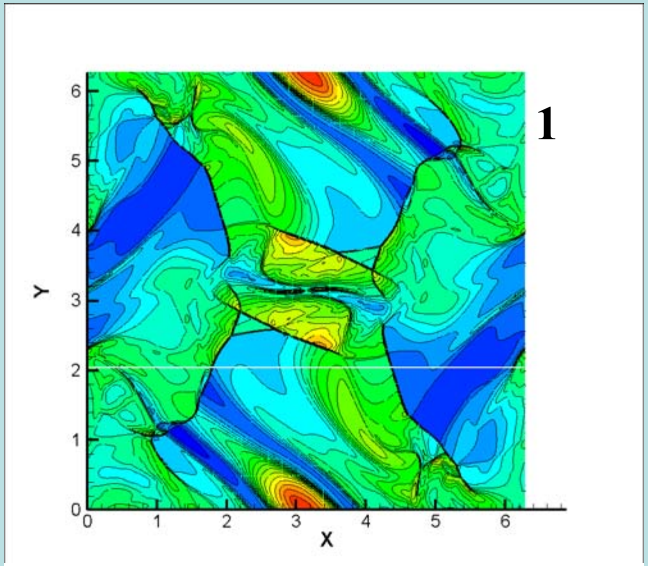

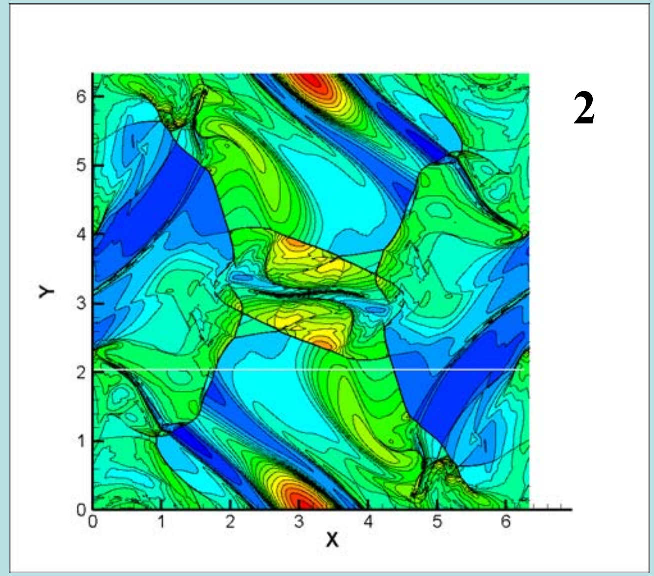

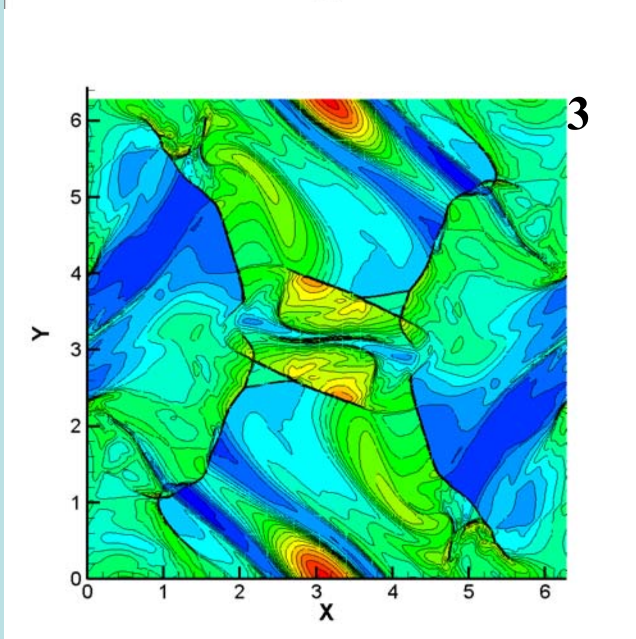

MS-FLUKSS with 8-wave source term only (1) and with the Poisson cleaning (3), and Sjogreen – Yee scheme (2).

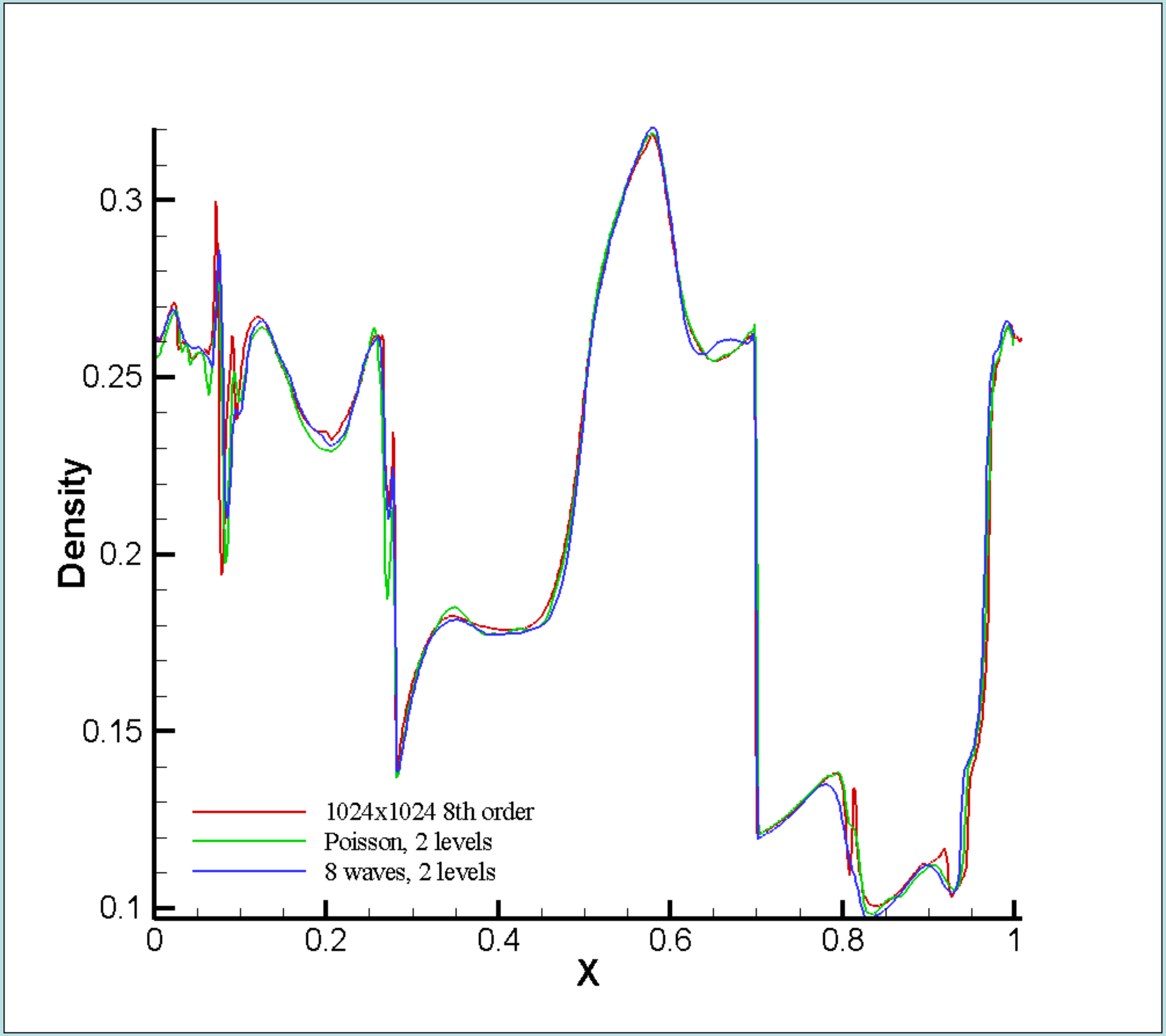

Density
0.3
0.25
0.2
0.15
0.1
0
0.2
0.4
0.6
0.8
1
X
1024x1024 8th order
Poisson, 2 levels
8 waves, 2 levels

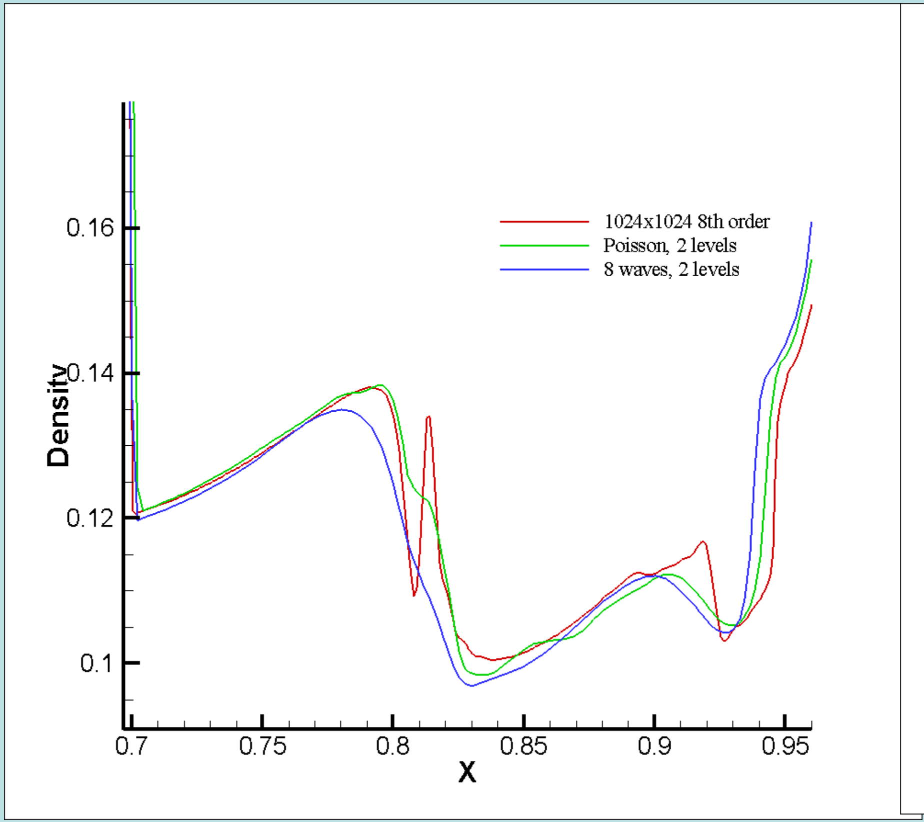
1024x1024 8th order
Poisson, 2 levels
8 waves, 2 levels
Density
0.16
0.14
0.12
0.1
0.7
0.75
0.8
0.85
0.9
0.95
X

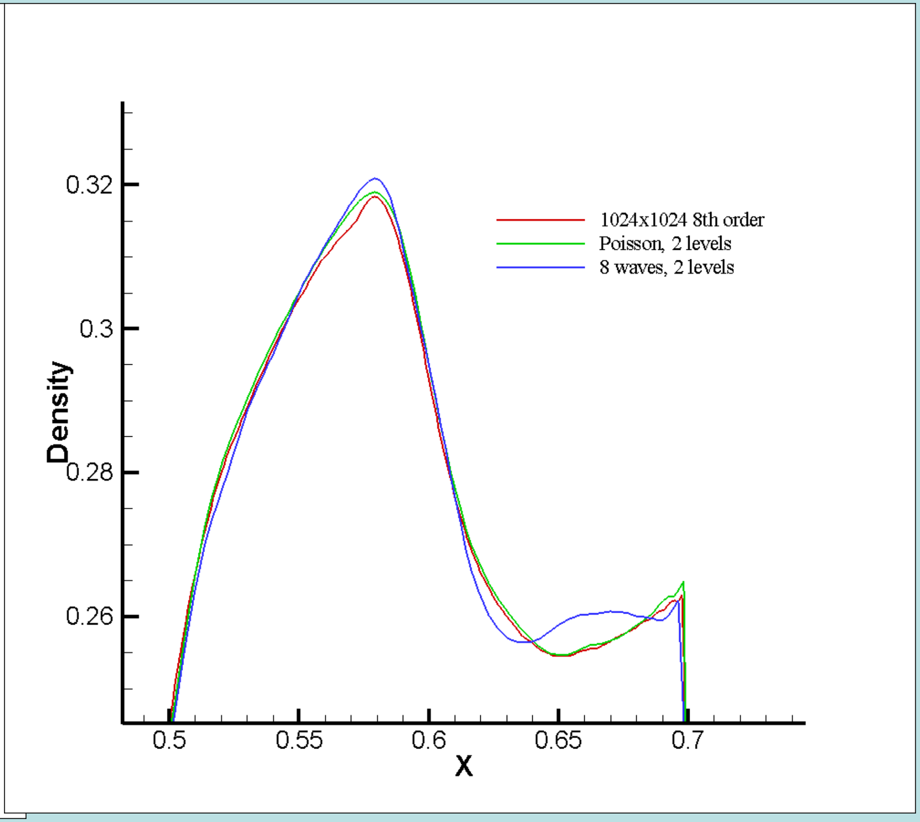
1024x1024 8th order
Poisson, 2 levels
8 waves, 2 levels
Density
0.32
0.3
0.28
0.26
0.5
0.55
0.6
0.65
0.7
X

ISMF in the HDP: Direction of the neutral hydrogen velocity in the inner heliosphere as a possible interstellar magnetic field compass

According to the SOHO SWAN experiment (Lallement et al, 2005), there is an angle of about 4° between the neutral He and neutral H flow velocity vectors in the inner heliosphere.

The vectors B_∞ and V_∞ define the *BV*-plane, which supposedly is nearly parallel to the HDP (Izmodenov et al. 2005). The angle between the HDP and the BV-plane can be ± 14º (Pogorelov et al., 2007).

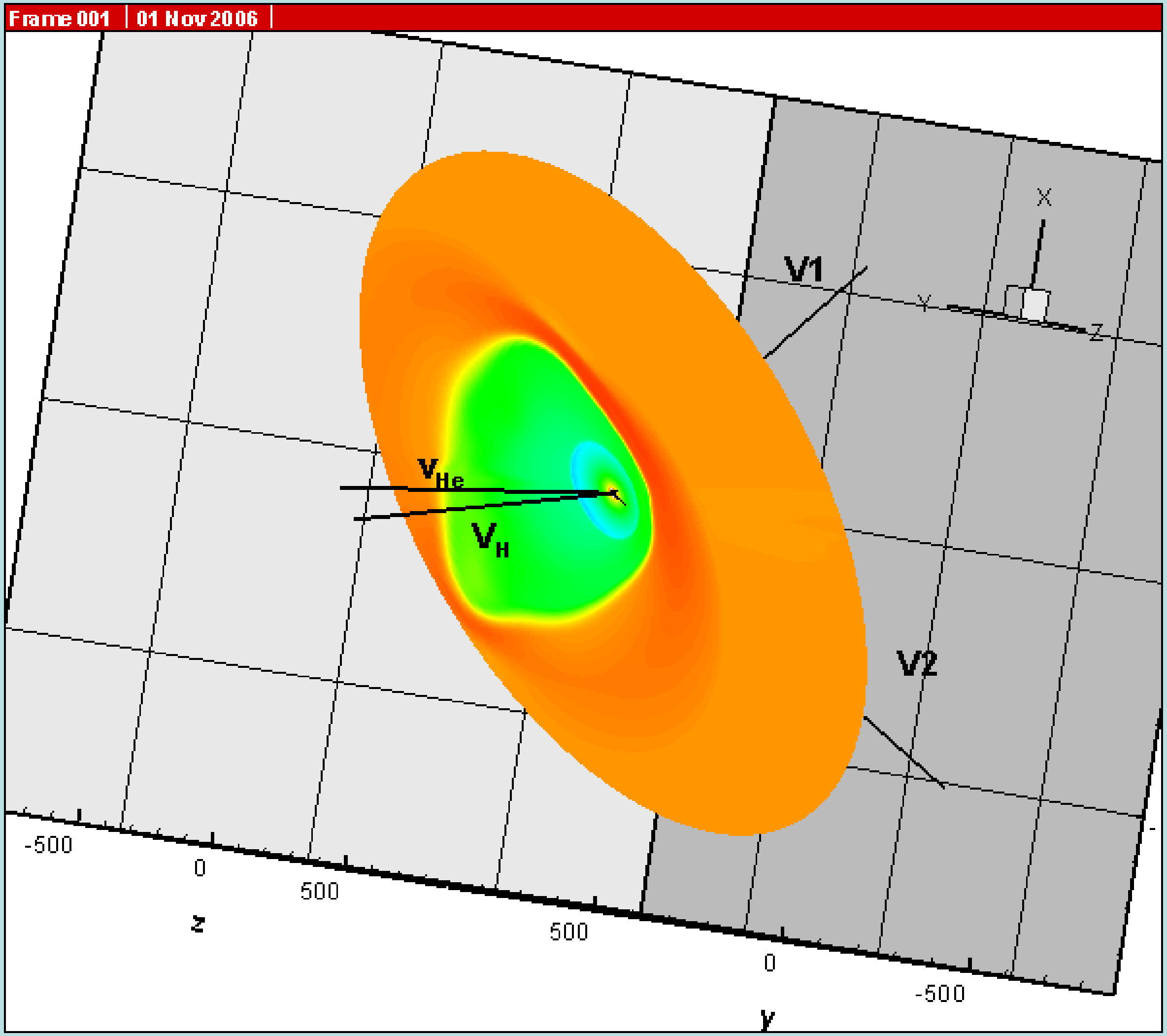

The heliopause colored by the sign of B_R, the hydrogen deflection plane, the Galactic plane, and the trajectories of the V1 and V2 spacecraft

Pogorelov, Heerikhuisen, Zank (2008)

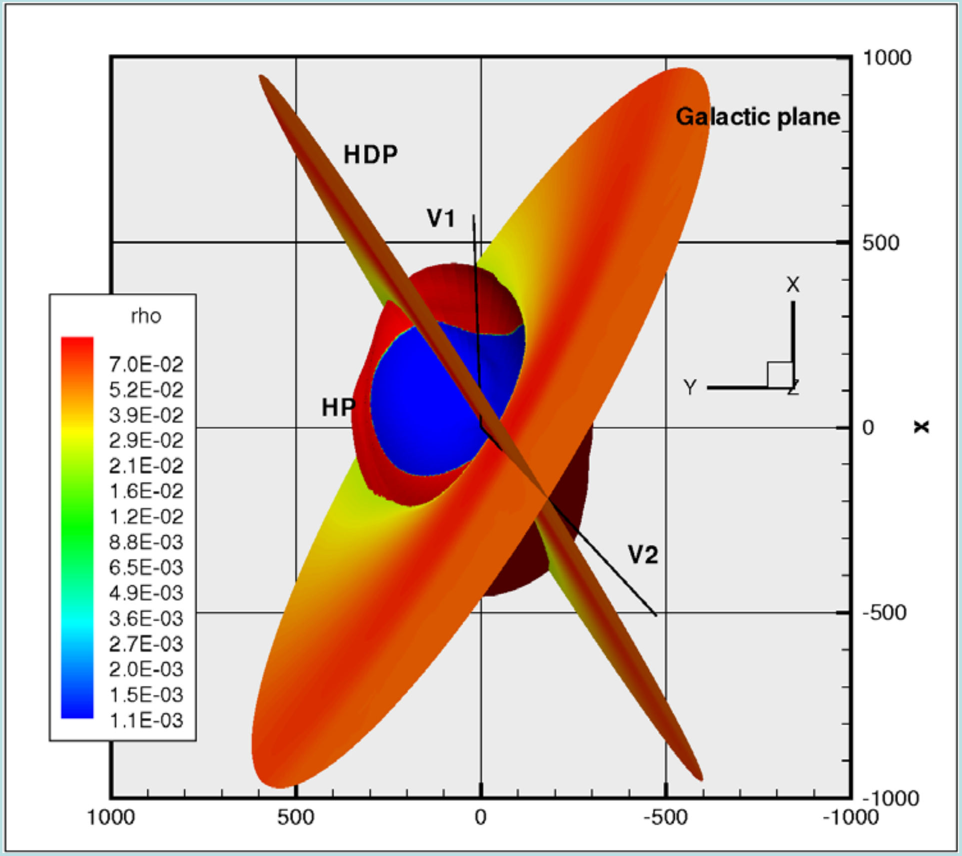

The HP is not symmetric with respect to the BV-plane!

***BV*-plane parallel to the HDP, B_∞ at 30° to V_∞ (B_∞ = 3 μG), $n_{H\infty}$ = 0.15 cm^{-3}**

Comparison of the neutral particle density distribution

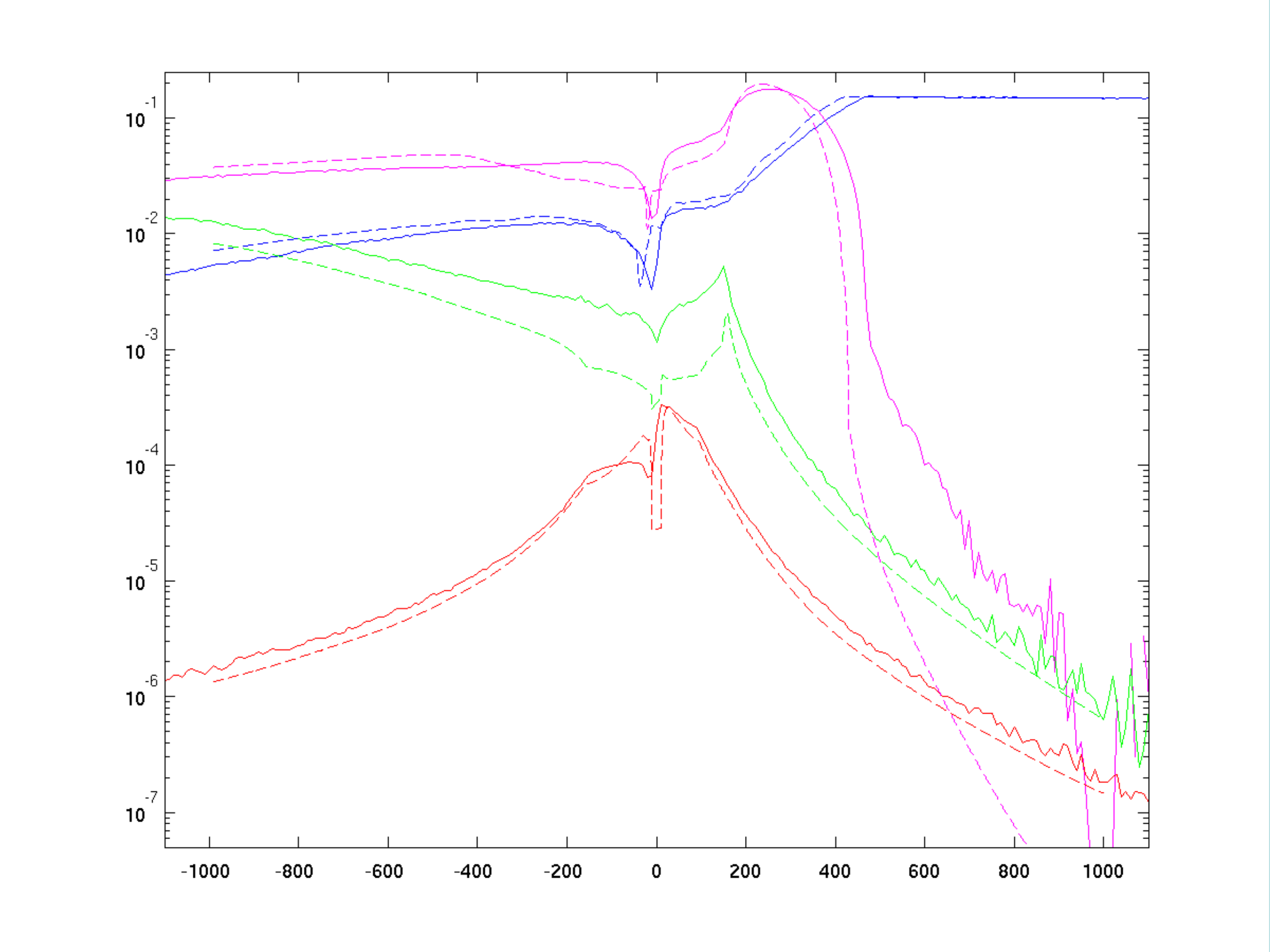

Population 0 (blue lines), 1 (purple lines), 2 (green lines), and 3 (red lines)

Plasma density distribution in the *V1-V2* plane for the ISMF strength 3 μG (left) and 4 μG (right)

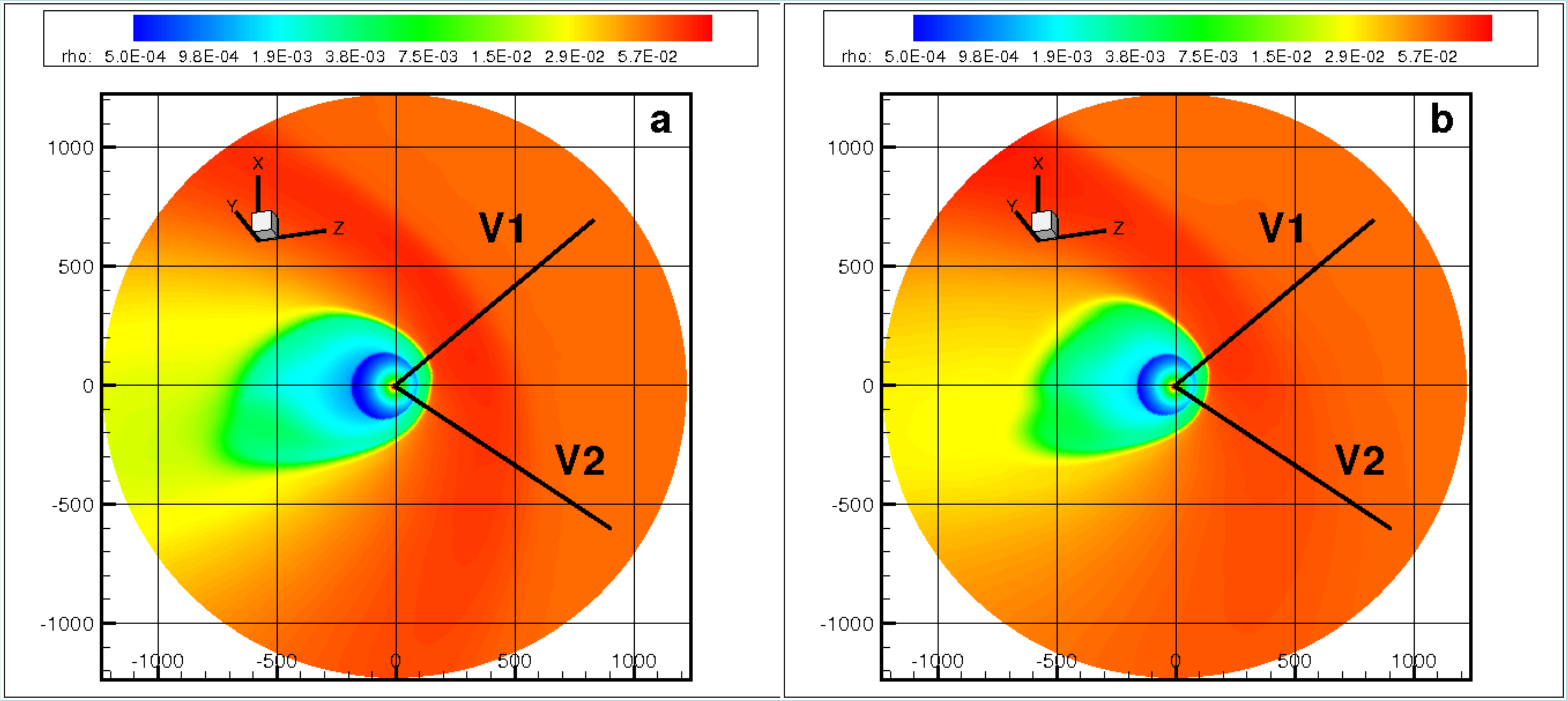

The TS heliocentric distance in the V2 direction is ~4 AU smaller than in the V1 direction for the former case and 9.5 AU smaller in the latter case (Pogorelov et al., 2009). The longitudinal asymmetry also substantially increases.

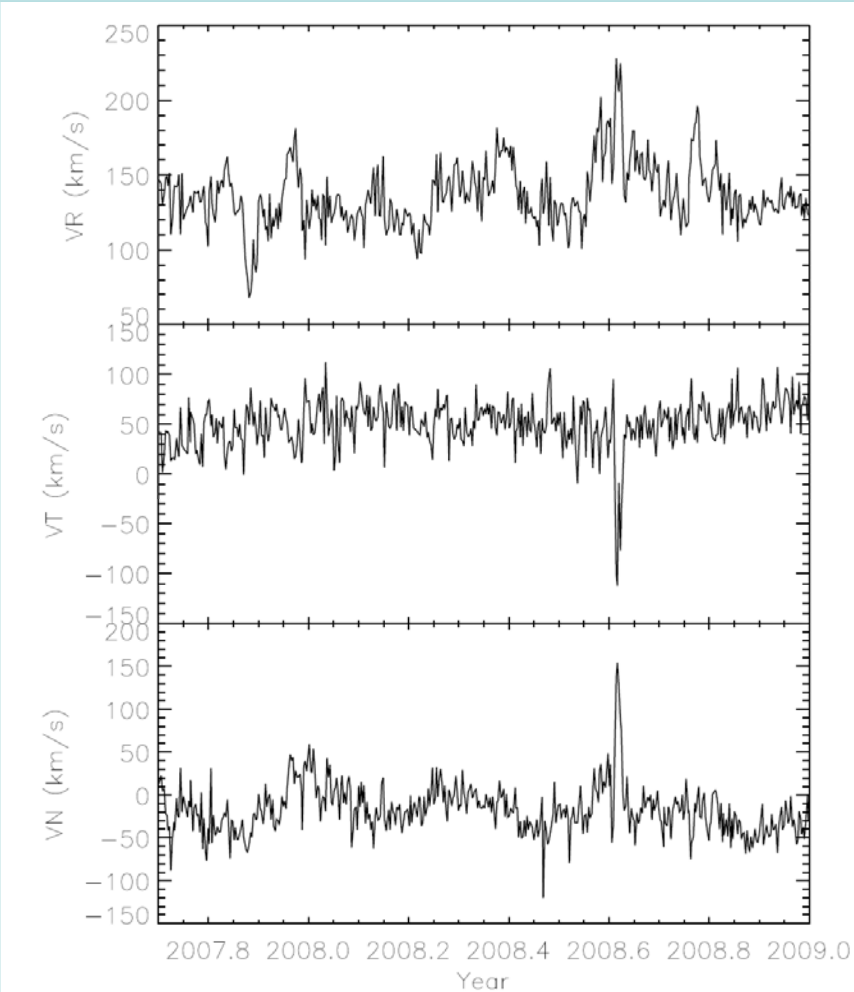

V2 data courtesy of John Richardson

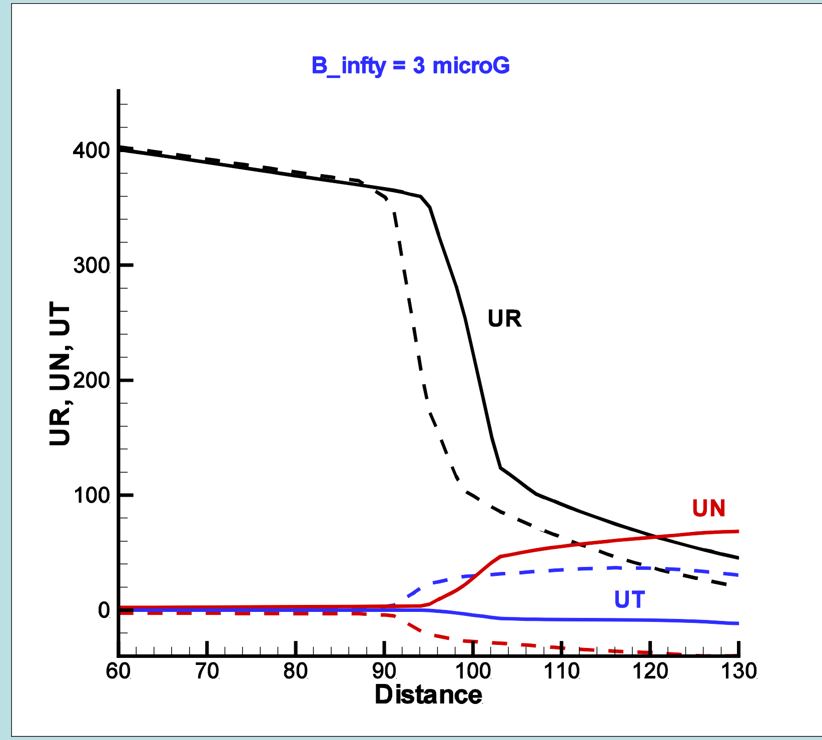

U_R is smaller (90 km/s vs. 138 km/s) than what is observed, and the calculated gradient is much larger (≈ -11 km/s/yr). UT is ≈ 35 km/s (48 km/s observation), and UN is ≈ -27 to -32 km/s within 10 AU from the TS (-14 km/s at 5 AU from V2).

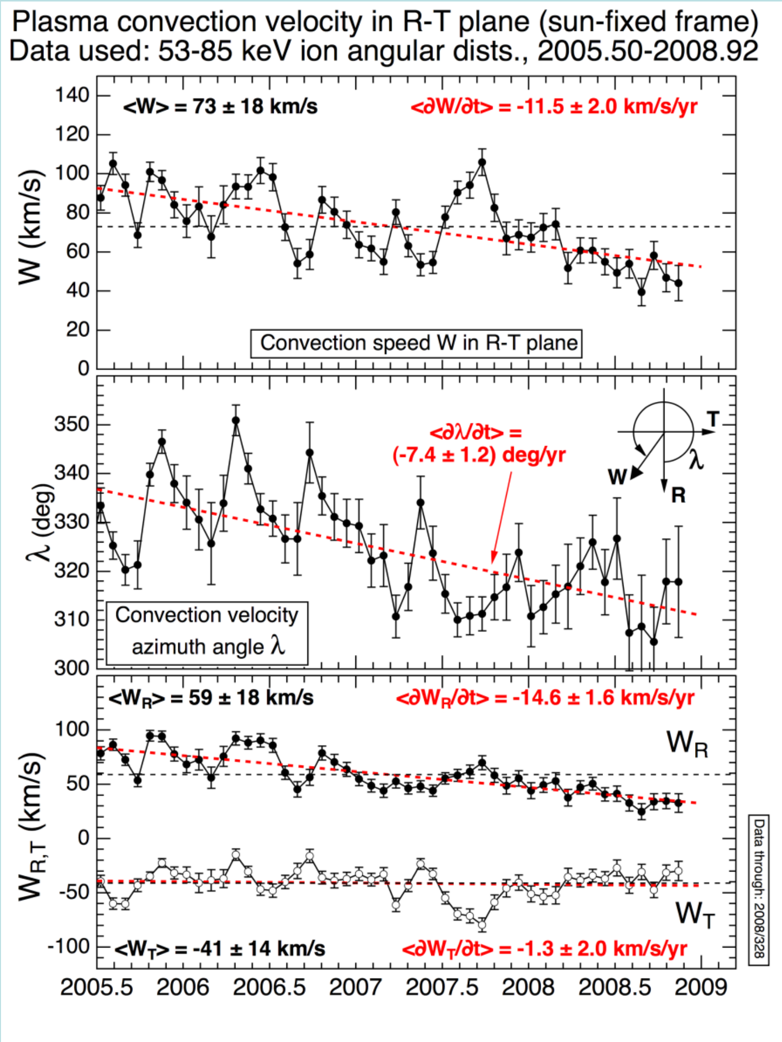

On the basis of our model calculations:
$dU_R/dt \approx -8.2$ km/s/yr,
$dU_T/dt \approx -0.6$ km/s/yr,
$dU_N/dt \approx +3.5$ km/s/yr,
(for $B_\infty = 3$ μG).

In both 3 μG and 4 μG cases U_R is consistently larger in the V1 direction than in the V2 direction at the same distance from the TS.

The distributions should probably be determined by unsteady phenomena: we need more realistic boundary conditions in the SW.

V1 observations courtesy of Rob Decker

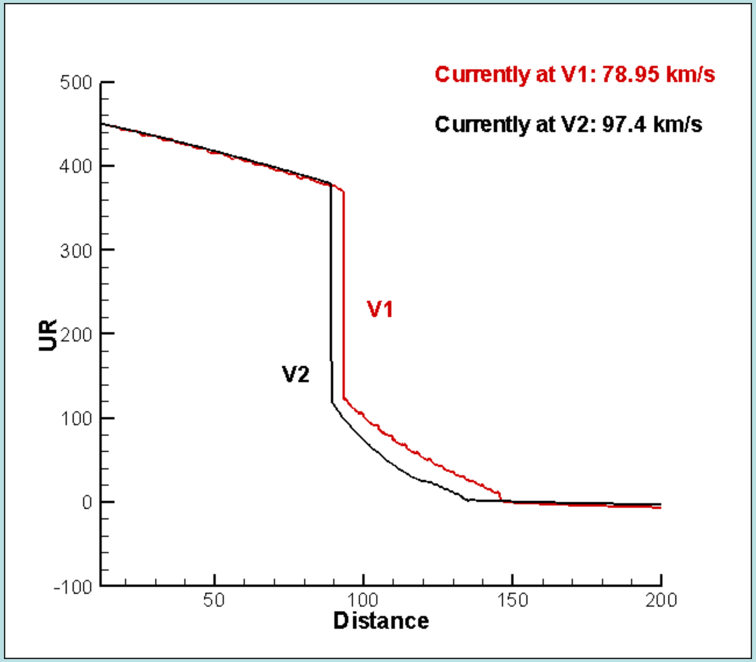

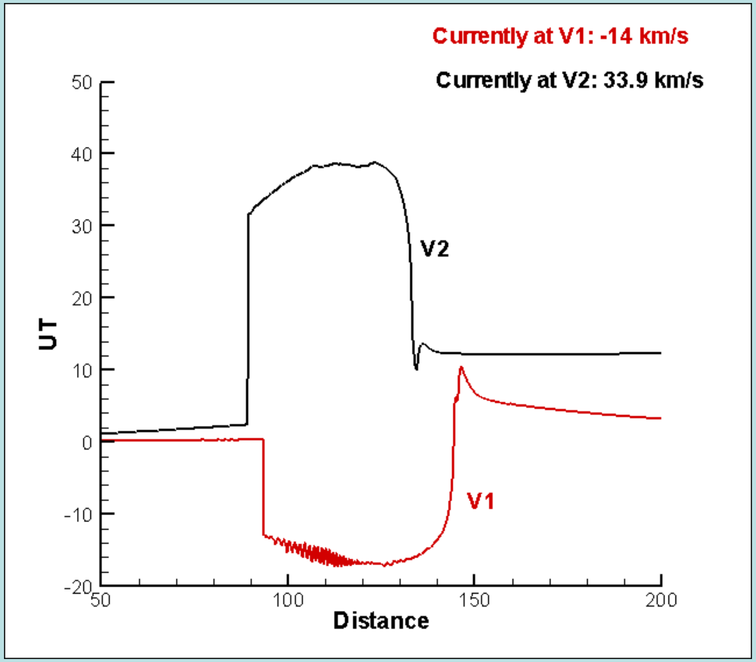

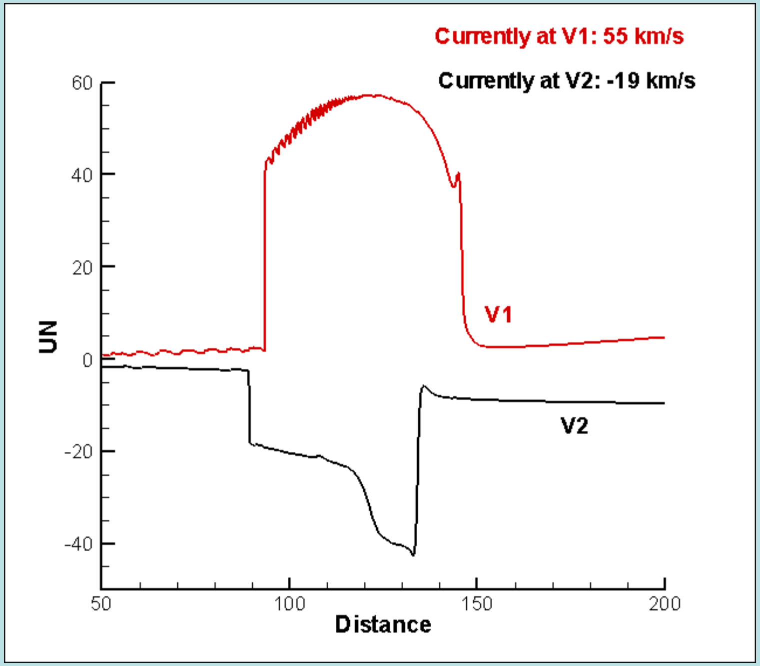

Voyager 1 (LECP): UR= 67 ± 16 km/s
UT= -42 ± 15 km/s.

Voyager 2 (PLS): UR= 138 km/s,
UT= 48 km/s, UN= -14 km/s.

With ISMF strength of 4 microG, the observed relationship between UR at V1 and V2 cannot be reproduced.

HCS in the supersonic SW. Ideal MHD model.

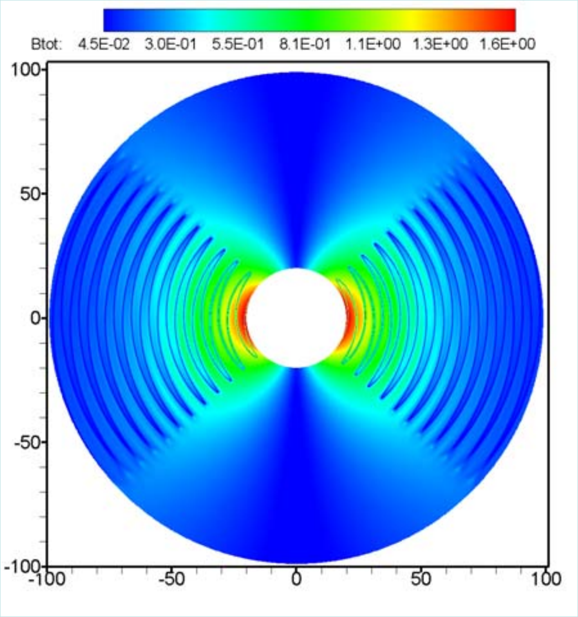

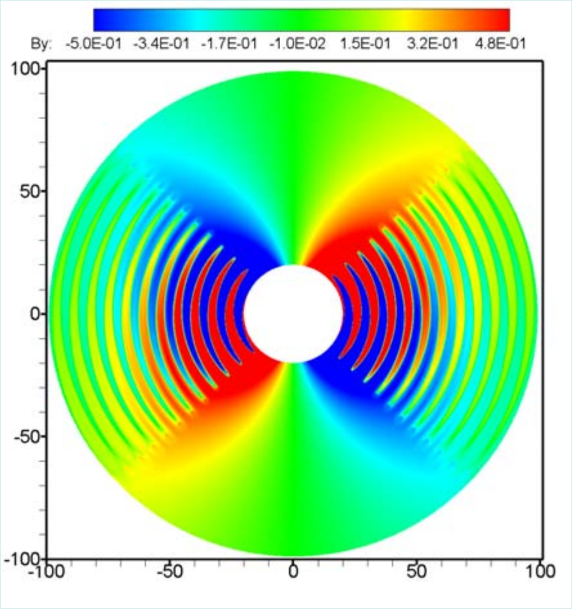

|**B**|, B_y, and U_R in the plane containing the Sun's rotation axis.

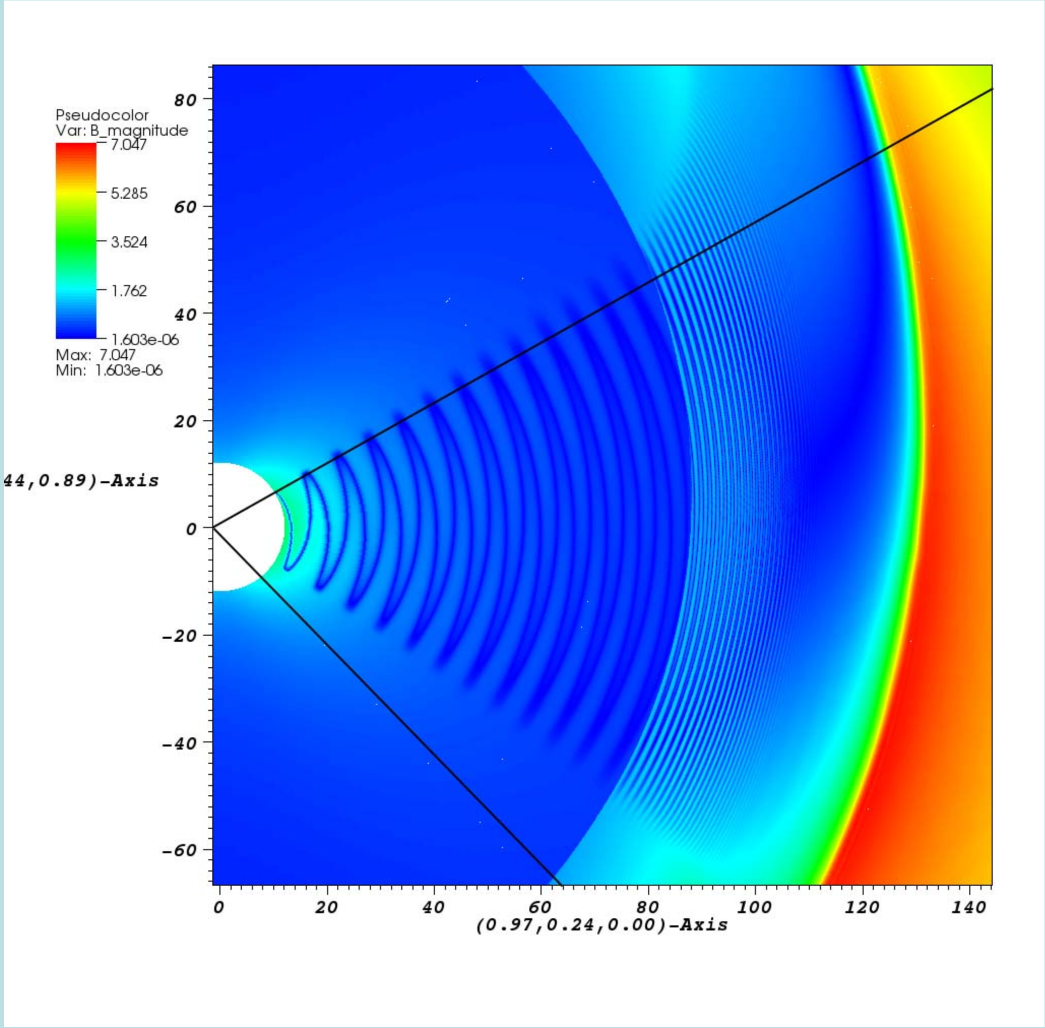

Sector structure can reappear in the heliosheath for V1.

Magnetic field distribution in the V1-V2 plane. The tilt of the Sun's dipole is 35º.

Calculated IMF gradients in the inner heliosheath along V1 trajectory

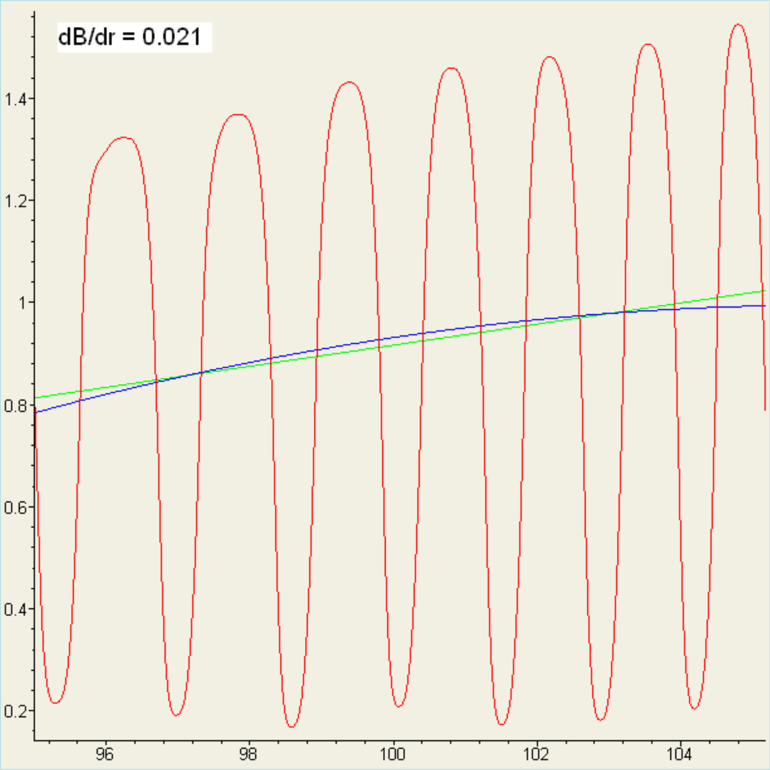

Burlaga et al. (2009) report grad B to be between 0.017 and 0.055 μG/AU.

Interaction of the periodic SW with the LISM

Slow SW

$$n_E = 8\,\mathrm{cm}^{-3}$$
$$V_E = 400\,\mathrm{km/s}$$
$$T_E = 10^5\ \mathrm{K}$$

Fast SW

$$n_E = 3.6\,\mathrm{cm}^{-3}$$
$$V_E = 800\,\mathrm{km/s}$$
$$T_E = 2.6\times10^5\ \mathrm{K}$$

The latitudinal extent of the slow SW changes periodically over 11 years from ± 35º at the solar minimum to ± 80º at the solar maximum. The tilt of the Sun's magnetic axis to its rotation axis changes from 9º at the solar minimum to 80º at the solar maximum. The IMF polarity changes to the opposite every 11 years at the maximum.

LISM: $n_\infty = 0.05\ \mathrm{cm}^{-3}$, $V_\infty = 26.4$ km/s, $T_\infty = 6527$ K, $B_\infty = 3\ \mu$G,
$n_{H\infty} = 0.15\ \mathrm{cm}^{-3}$

$\mathbf{B}_\infty$ belongs to the RL plane directed at 30º to $\mathbf{V}_\infty$, which is at 5º to the ecliptic plane.

Evolution of the magnetic field magnitude in the meridional plane

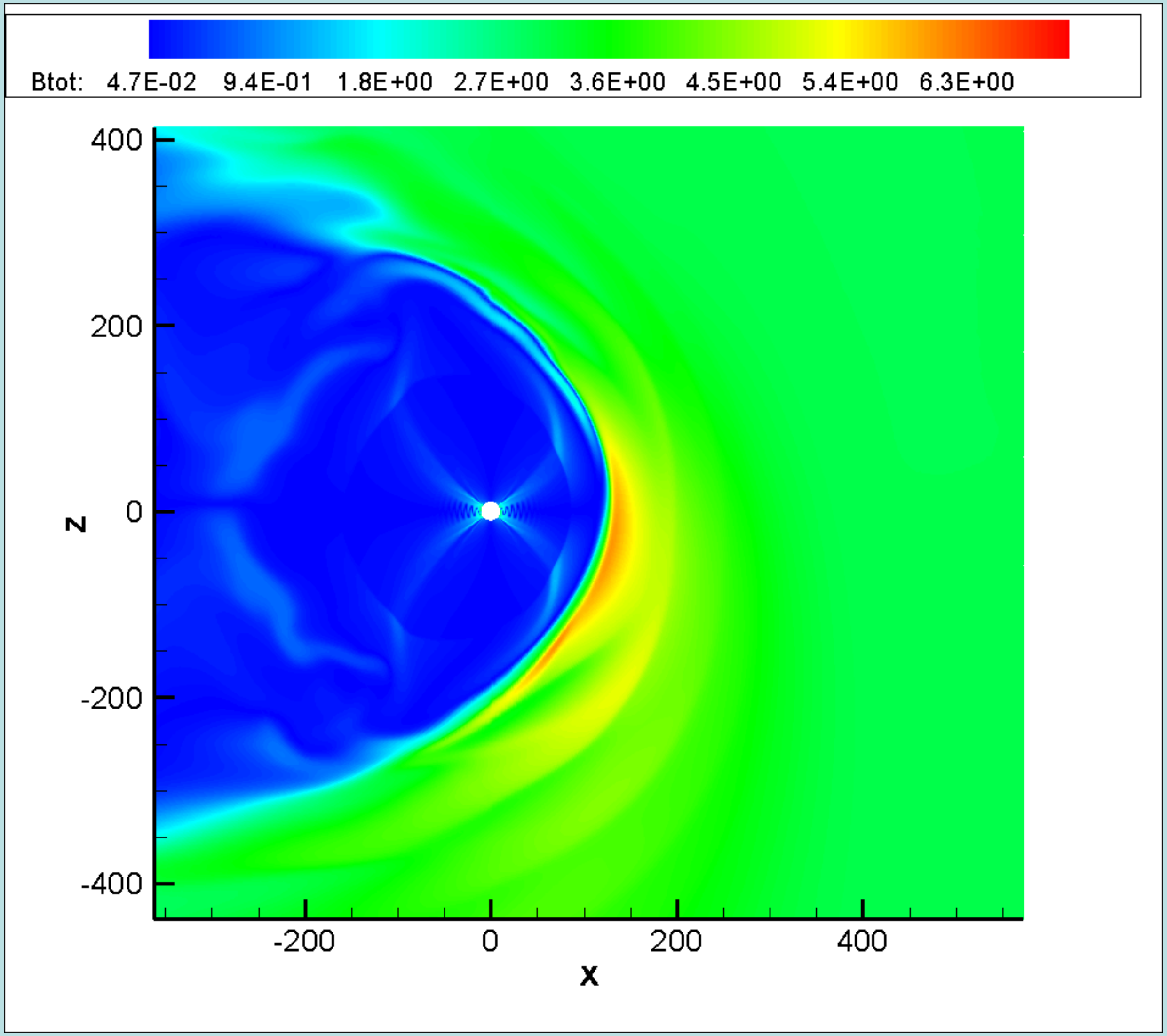

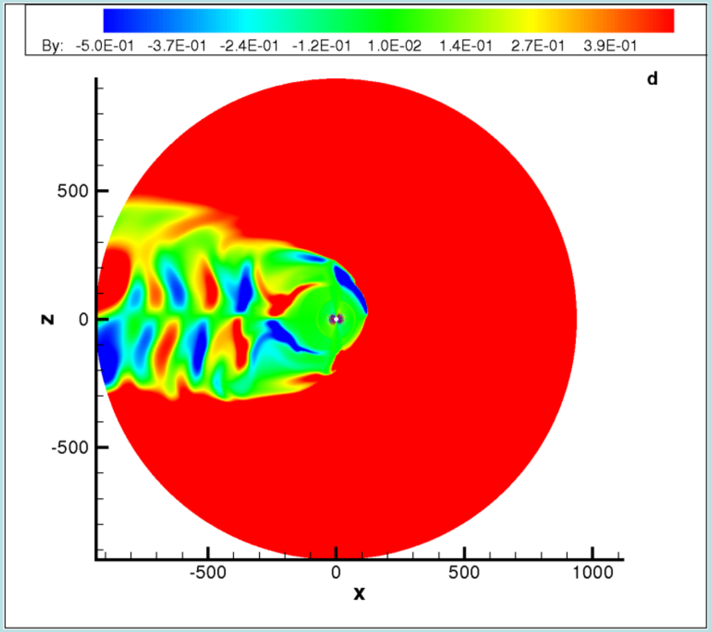

B_y (out-of-plane) time evolution over the solar cycle

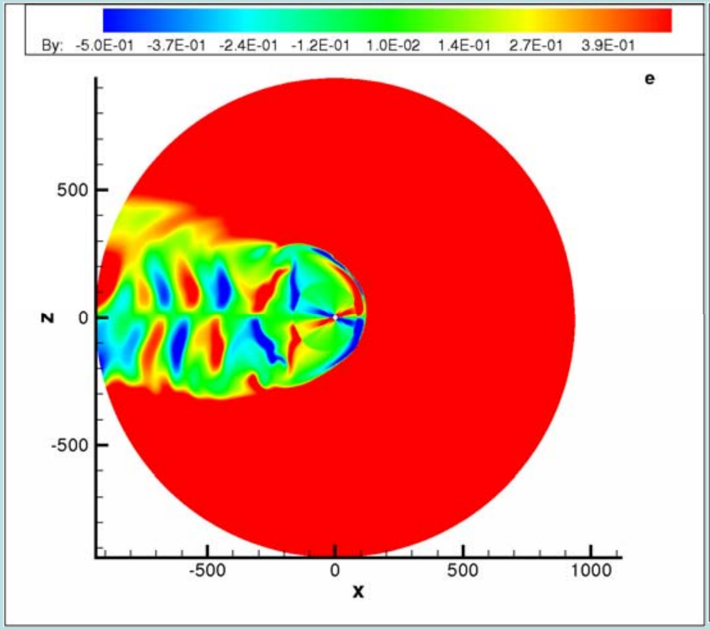

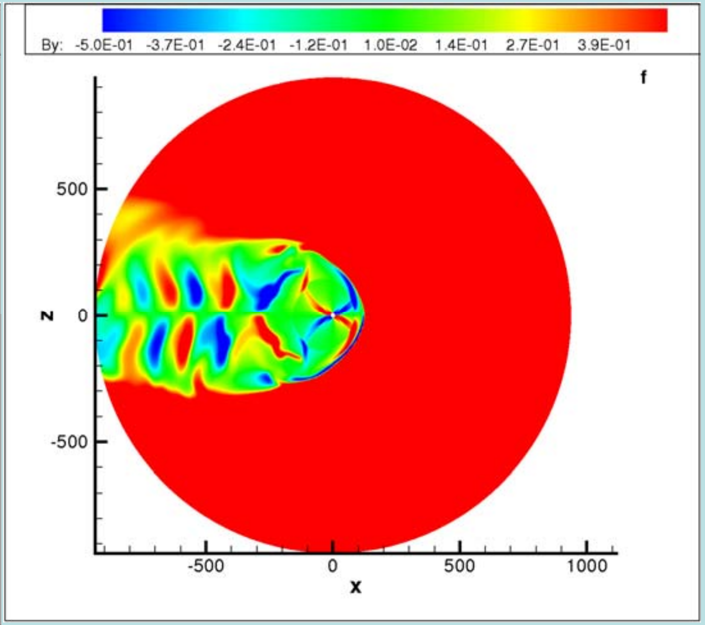

Space-time distributions of the plasma quantities in the direction roughly corresponding to the V2 trajectory

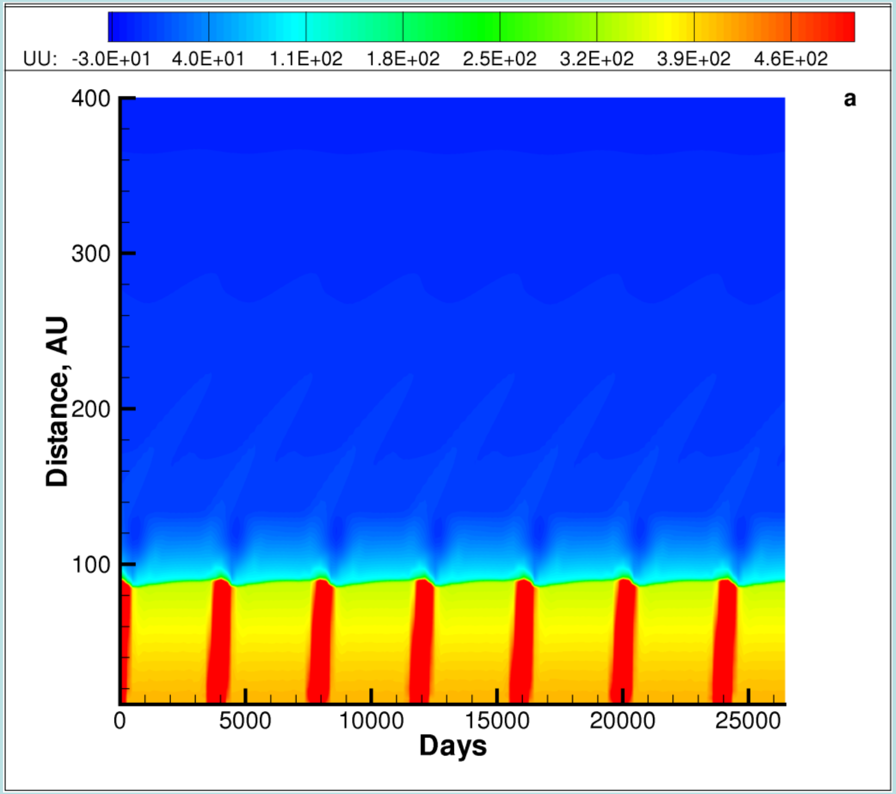

Radial component of the velocity vector

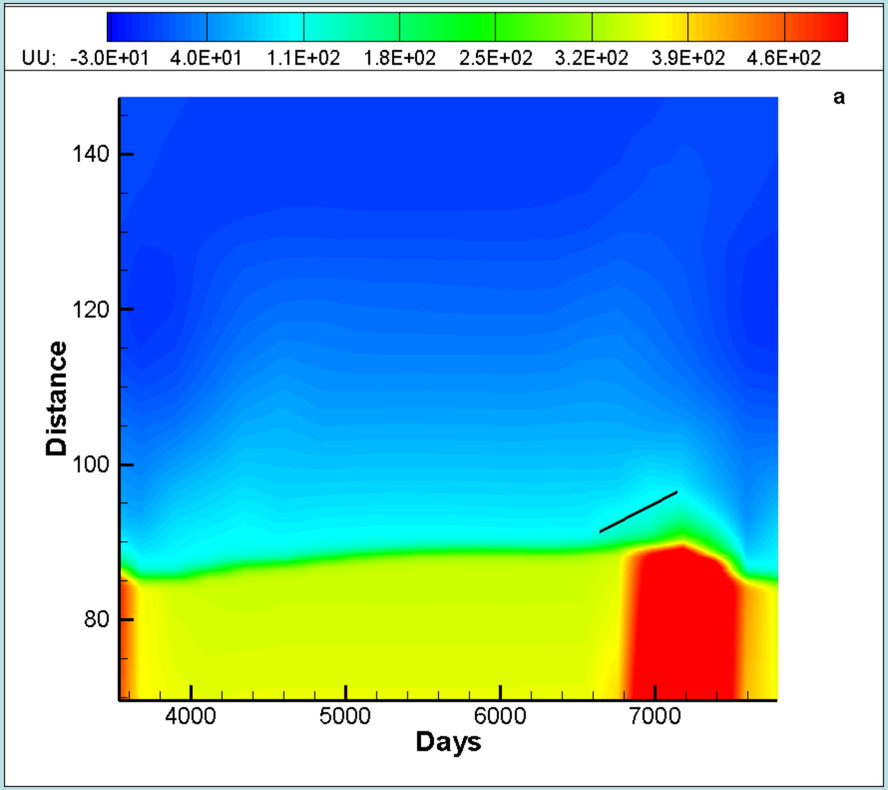

The V2 trajectory is a straight line in this plot. The radial component of the SW velocity can remain nearly constant for some time if V2 is surfing along the boundary between slow and fast SW regions.

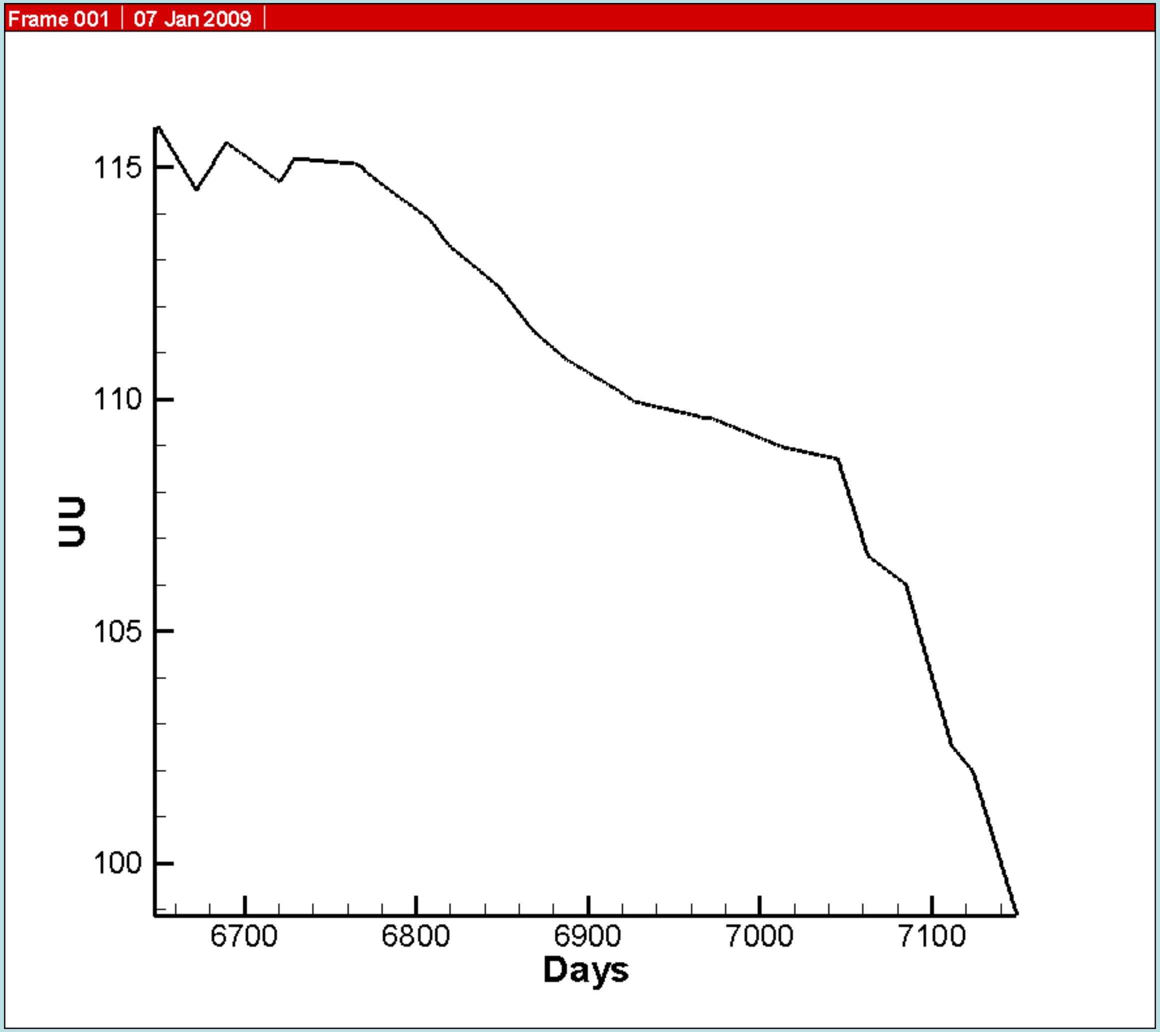

SW radial velocity component roughly in the V2 direction.

SW radial velocity and H^+ density at 10 AU for the solar minima determined by the first and third Ulysses pole-to-pole flybys.

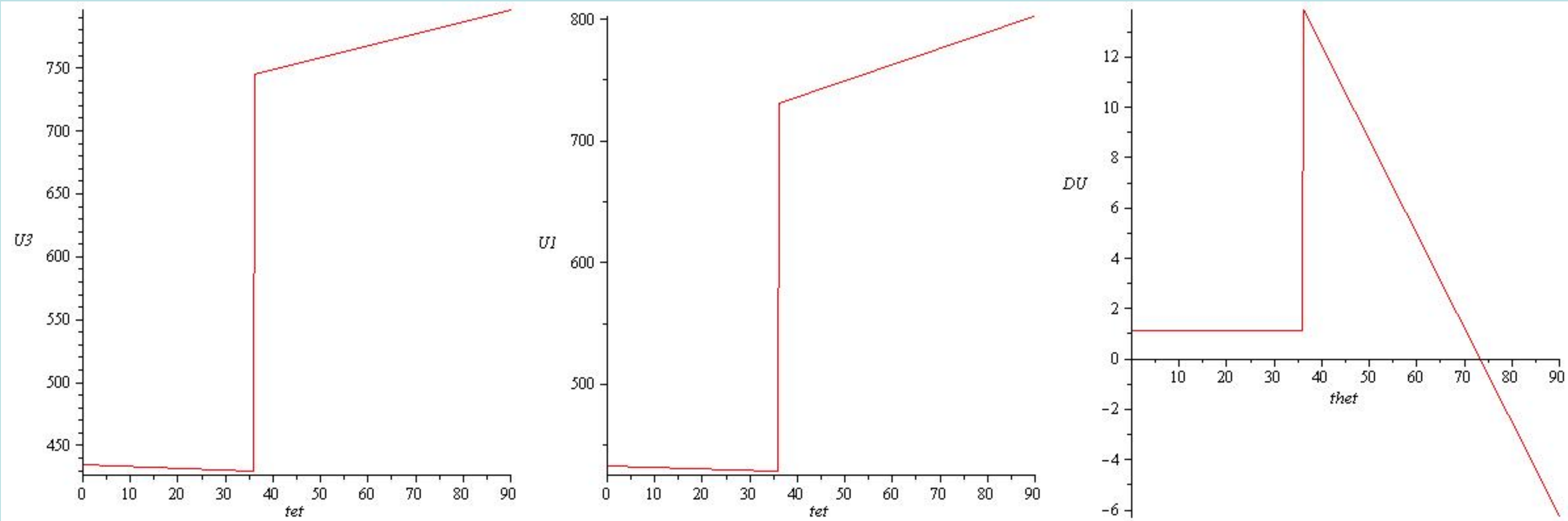

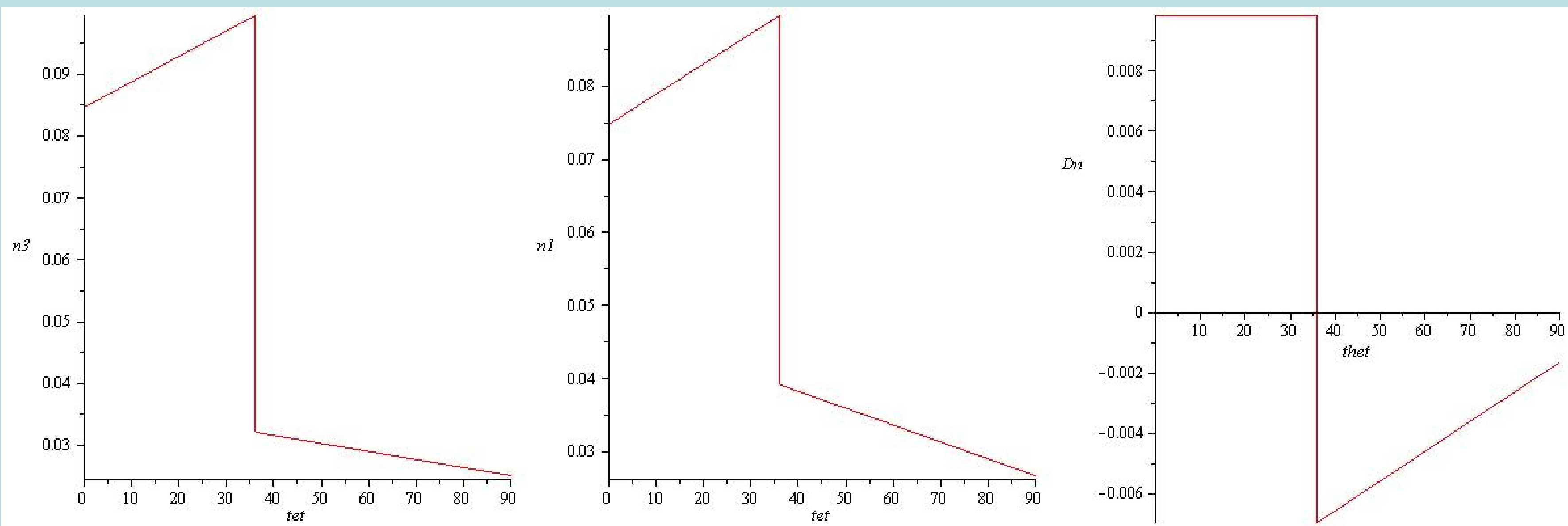

Plasma density in the V1-V2 plane for the minima derived from the 1st and 3rd Ulysses pole-to-pole flybys.

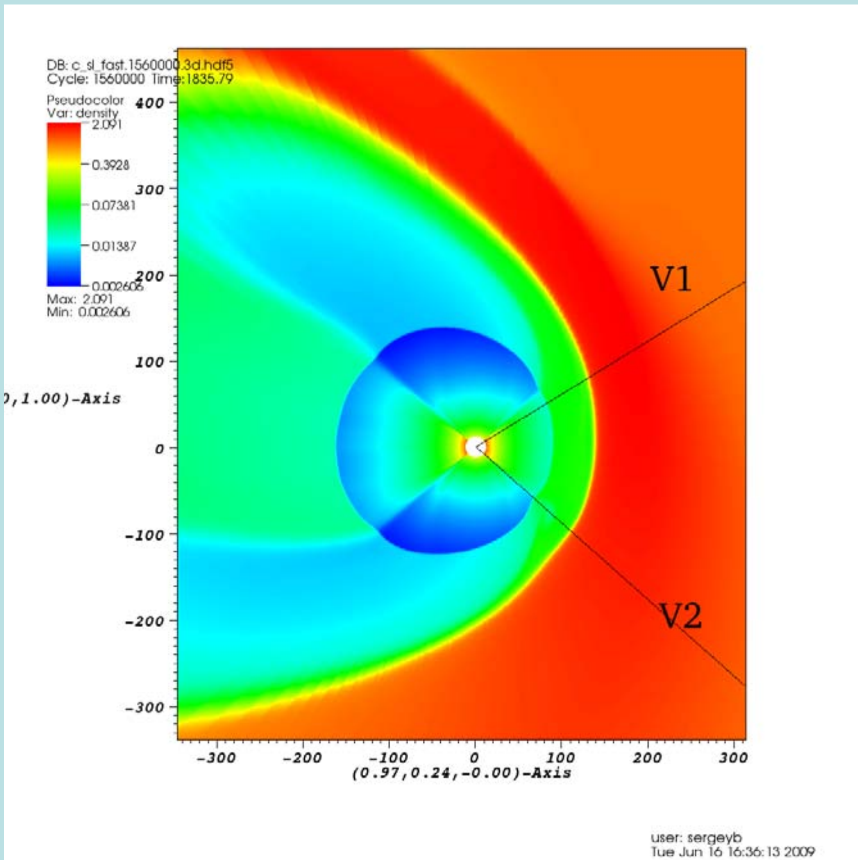

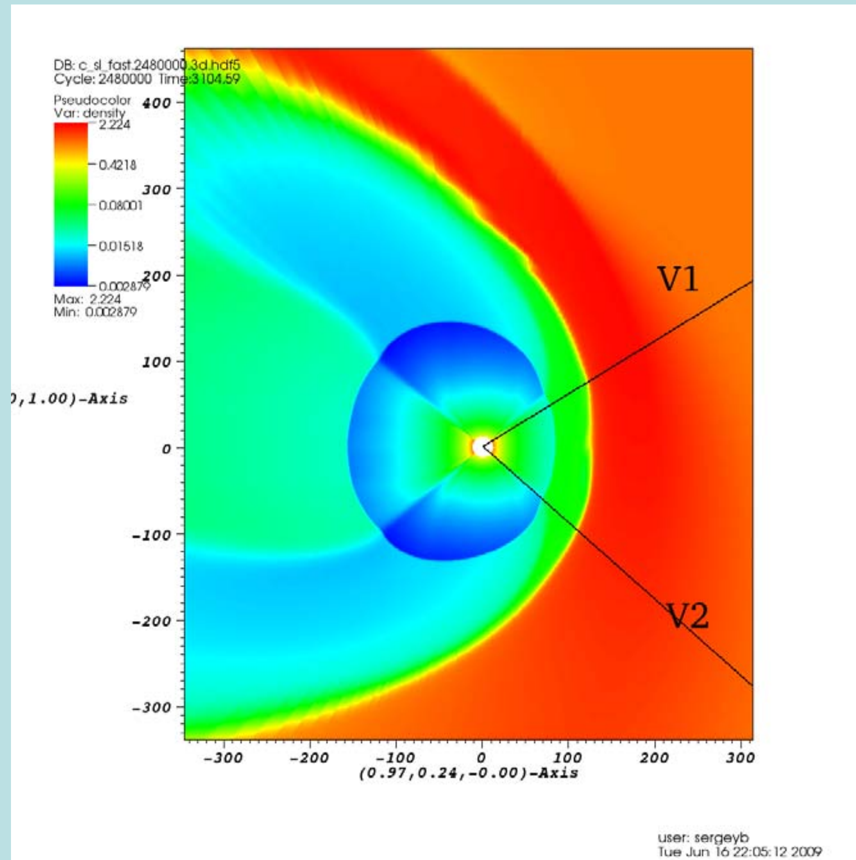

CONCLUSIONS

1. **Developed in the UAH/CSPAR, MS-FLUKSS proved to be an efficient tool for modeling multi-scale heliospheric flows.**
2. **Improvements are necessary to allow for multi-core processor architectures.**
3. **Higher-order numerical methods might be useful for modeling shock-turbulence interaction.**
4. **Time-dependent b. c. at 1 AU are essential for comparison with Voyager measurements. However, they are, on the one hand, incomplete and, on hand, too detailed for global modeling, merging by 20 AU.**
5. **Kinetic treatment of pick-up ions is required, being especially complicated at the TS, where the distribution function becomes anisotropic.**

GMIR propagation

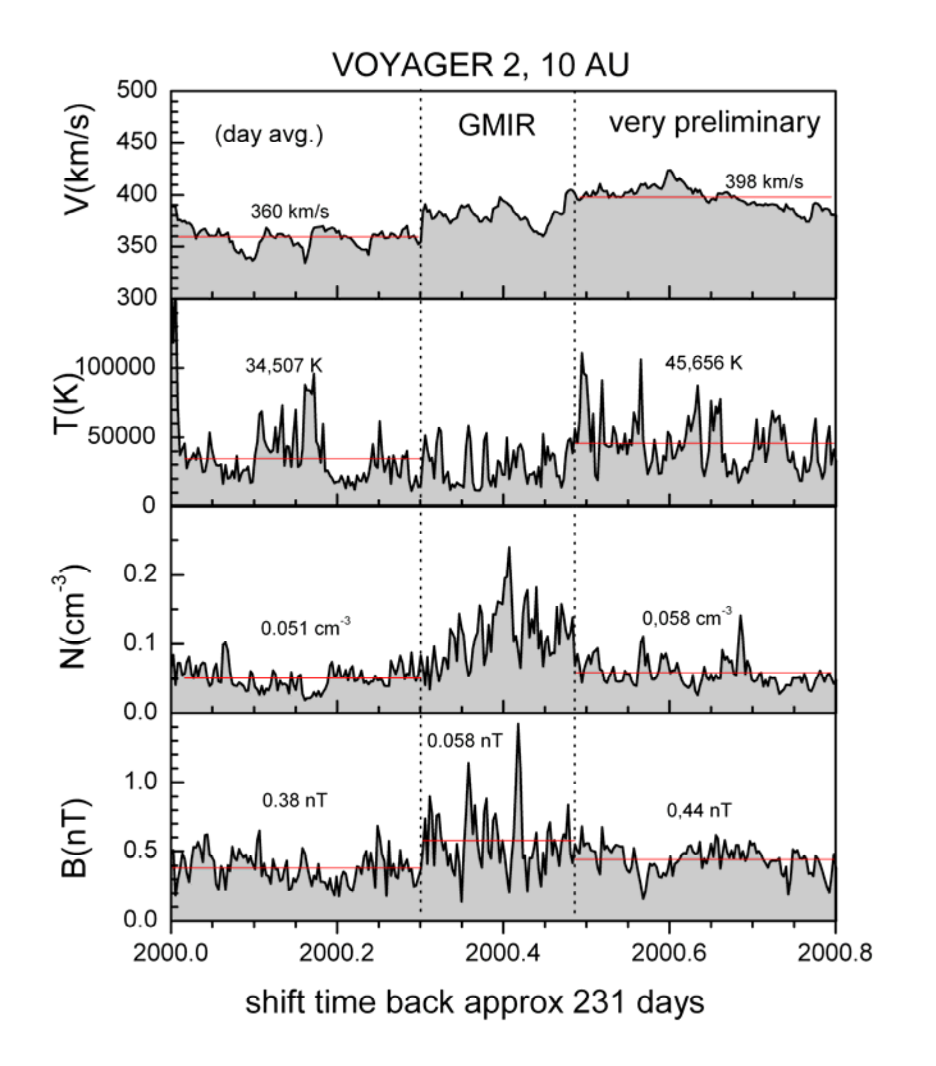

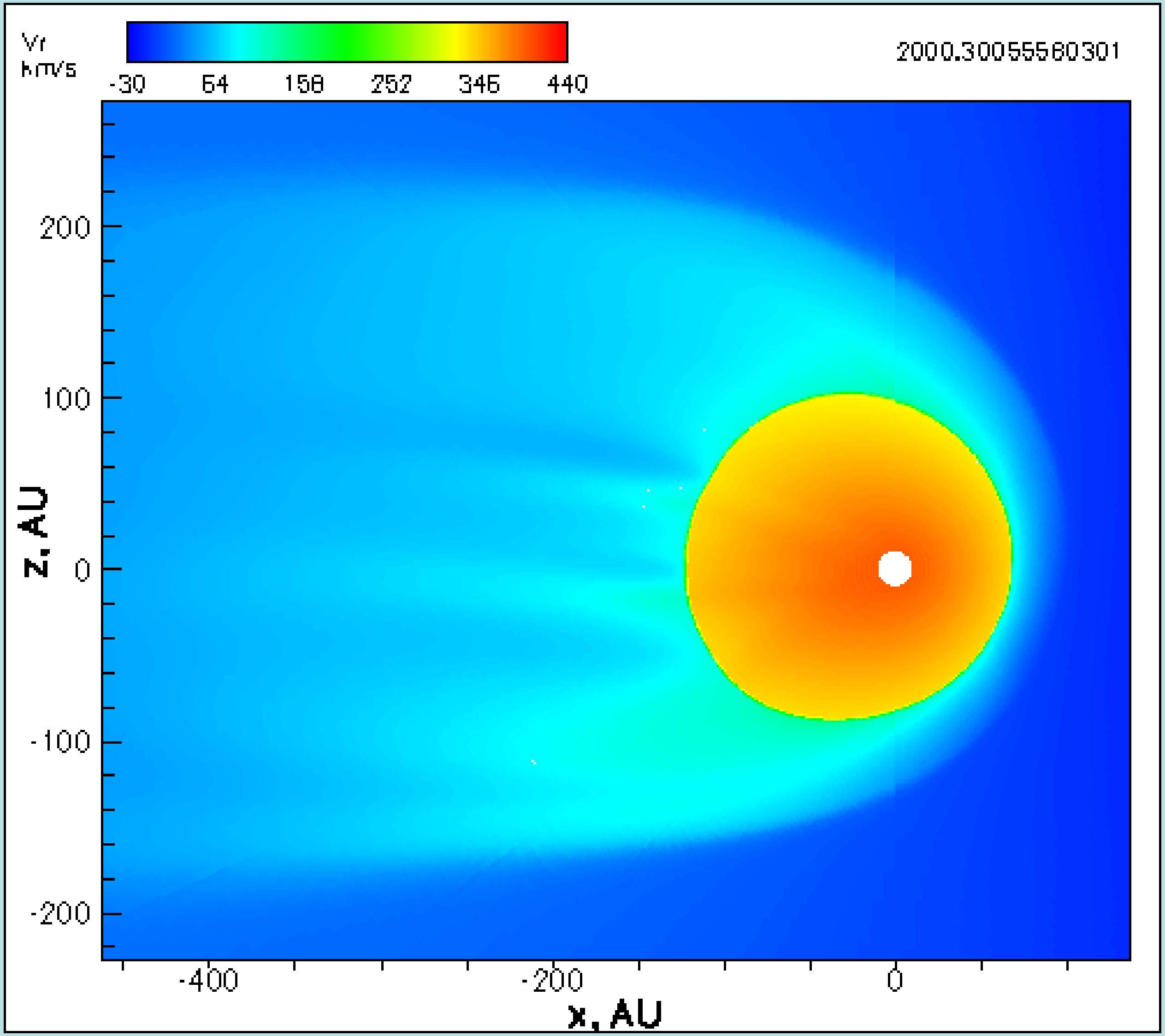

Radial velocity variation

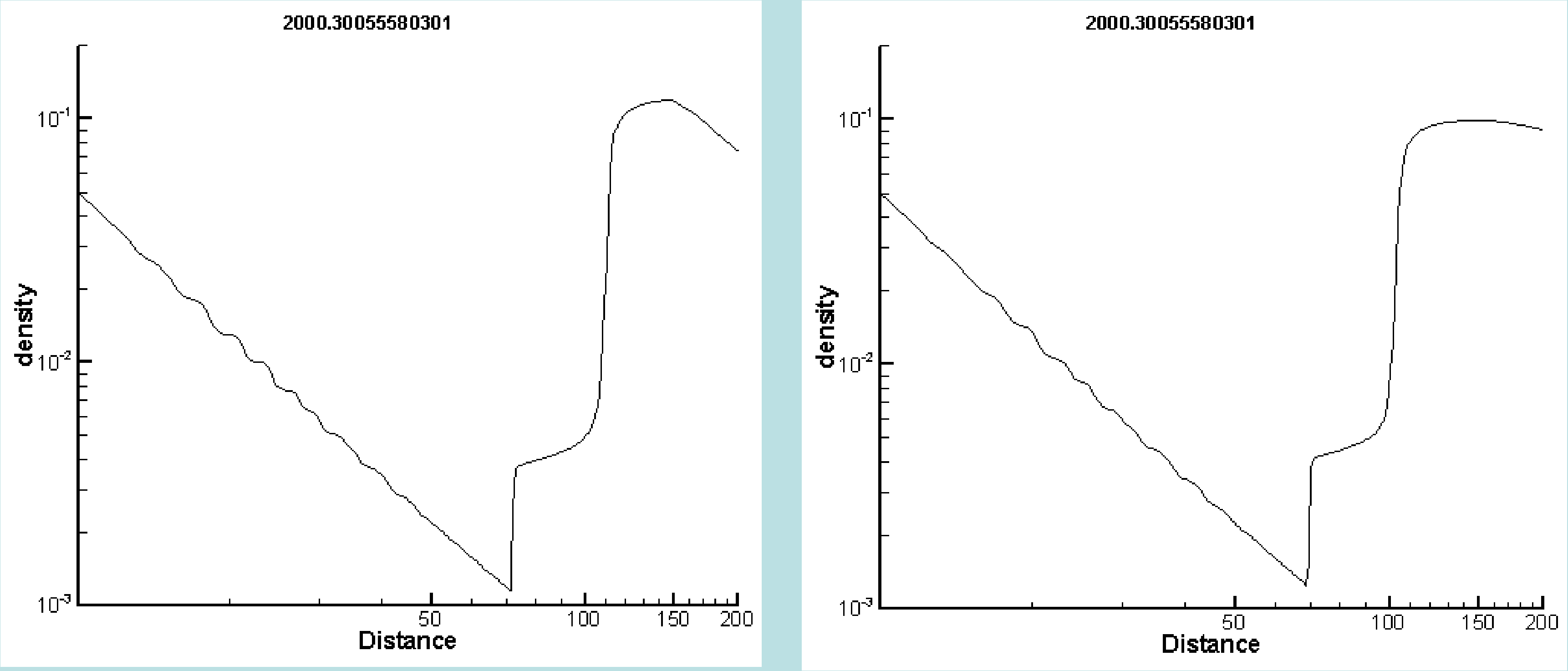

Plasma density variation in the V1 and V2 directions.

Entropy wave $A_e = 0.25$, $\alpha = 90°$, $\psi=60°$, $k_y=5$

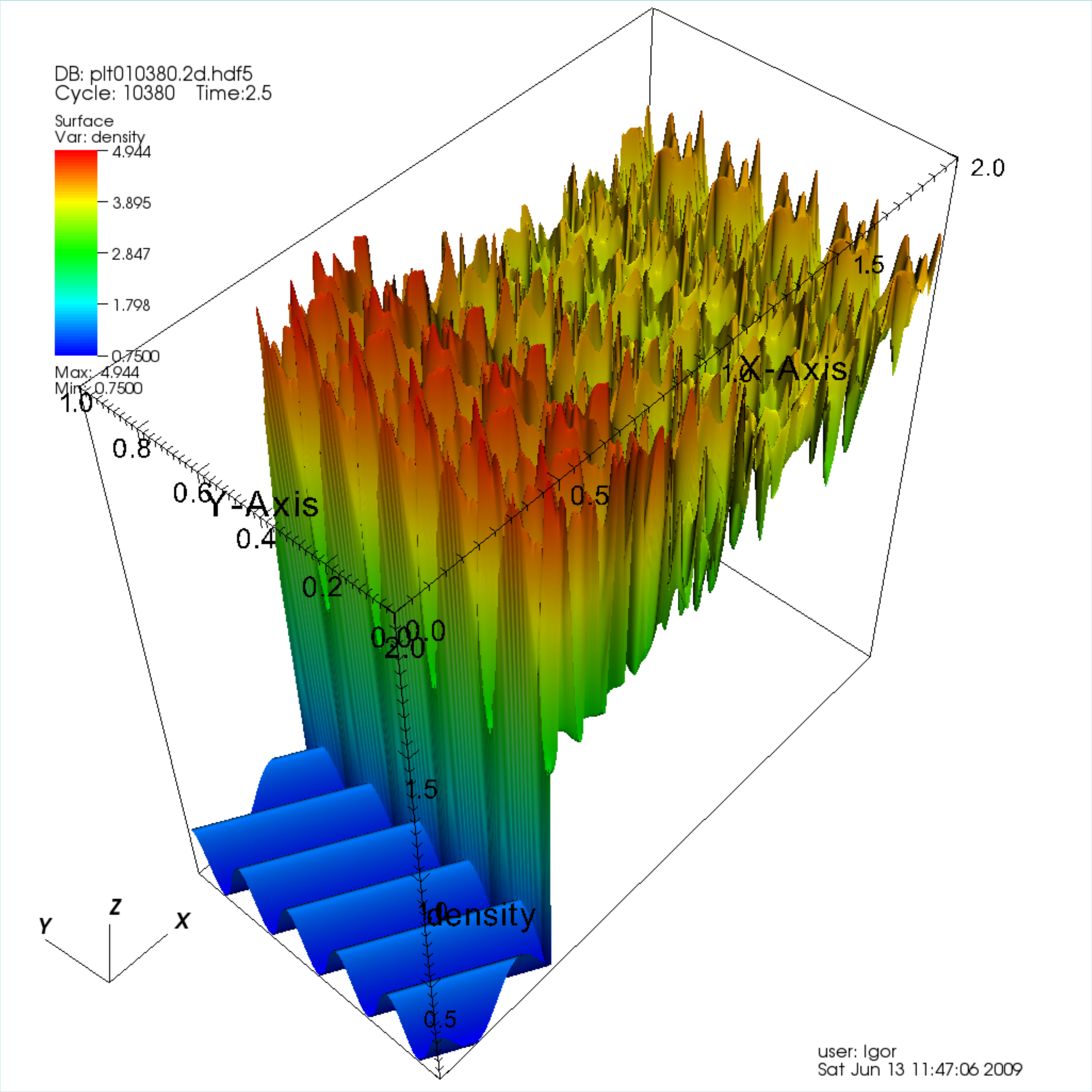

Density distribution